

## Regulated extravascular microenvironment *via* reversible thermosensitive hydrogel for inhibiting calcium influx and vasospasm

Binfan Zhao<sup>a,1</sup>, Yaping Zhuang<sup>b,1</sup>, Zhimo Liu<sup>a</sup>, Jiayi Mao<sup>a</sup>, Shutong Qian<sup>a</sup>, Qiuyu Zhao<sup>a</sup>, Bolun Lu<sup>a</sup>, Xiyuan Mao<sup>a</sup>, Liucheng Zhang<sup>a</sup>, Yuguang Zhang<sup>a,\*\*</sup>, Wenguo Cui<sup>b,\*</sup>, Xiaoming Sun<sup>a,\*\*\*</sup>

<sup>a</sup> Department of Plastic and Reconstructive Surgery Shanghai Ninth People's Hospital Shanghai JiaoTong University School of Medicine, 639 Zhi Zao Ju Road, Shanghai, 200011, PR China

<sup>b</sup> Department of Orthopaedics, Shanghai Key Laboratory for Prevention and Treatment of Bone and Joint Diseases, Shanghai Institute of Traumatology and Orthopaedics Ruijin Hospital Shanghai Jiao Tong University School of Medicine, 197 Ruijin 2nd Road, Shanghai, 200025, PR China

### ARTICLE INFO

#### Keywords:

Reversible thermosensitive hydrogel  
Low temperature response  
Calcium influx  
Vasospasm  
Vascular

### ABSTRACT

Arterial vasospasm after microsurgery can cause severe obstruction of blood flow manifested as low tissue temperature, leading to tissue necrosis. The timely discovery and synchronized treatment become pivotal. In this study, a reversible, intelligent, responsive thermosensitive hydrogel system is constructed employing both the gel–sol transition and the sol–gel transition. The “reversible thermosensitive (RTS)” hydrogel loaded with verapamil hydrochloride is designed to dynamically and continuously regulate the extravascular microenvironment by inhibiting extracellular calcium influx. After accurate implantation and following *in situ* gelation, the RTS hydrogel reverses to the sol state causing massive drug release to inhibit vasospasm when the tissue temperature drops to the predetermined transition temperature. Subsequent restoration of the blood supply alleviates further tissue injury. Before the temperature drops, the RTS hydrogel maintains the gel state as a sustained-release reservoir to prevent vasospasm. The inhibition of calcium influx and vasospasm *in vitro* and *in vivo* is demonstrated using vascular smooth muscle cells, mice mesenteric arterial rings, and vascular ultrasonic Doppler detection. Subsequent animal experiments demonstrate that RTS hydrogel can promote tissue survival and alleviate tissue injury responding to temperature change. Therefore, this RTS hydrogel holds therapeutic potential for diseases requiring timely detection of temperature change.

### 1. Introduction

Arterial vasospasm is a common complication after anastomosis in microsurgery, leading to lumen stenosis and micro thrombosis, and the occurrence of arterial vasospasm may cause ischemic necrosis of the transplanted tissue and lead to failure of the operation [1]. The continued monitoring of compromised circulation is critical after surgery [2,3]. The drop in temperature of the transplanted tissue is an essential manifestation of vascular compromise caused by vasospasm. Therefore, it is of great significance to promptly monitor this temperature change and address it to prevent the necrosis of the transplanted

tissue [4,5]. At present, temperature monitoring mainly relies on manual measurement, and it is challenging to detect temperature changes and provide effective interventions promptly [3,6]. Therefore, the timely discovery and synchronized treatment of the postoperative temperature change in transplanted tissue is the key to solving this problem.

Intelligent, responsive polymer biomaterials can dynamically rearrange their structure and perform “on-off” switching when small changes are detected in the environment to adapt to different needs [7–11]. Among them, intelligent thermoresponsive polymers are widely used for easy preparation, processing, and unrestricted modification [8,

Peer review under responsibility of KeAi Communications Co., Ltd.

\* Corresponding author.

\*\* Corresponding author.

\*\*\* Corresponding author.

E-mail addresses: [zhangyg18@126.com](mailto:zhangyg18@126.com) (Y. Zhang), [wgcui80@hotmail.com](mailto:wgcui80@hotmail.com) (W. Cui), [drsunxm@126.com](mailto:drsunxm@126.com) (X. Sun).

<sup>1</sup> These authors contributed equally to this work.

<https://doi.org/10.1016/j.bioactmat.2022.08.024>

Received 12 May 2022; Received in revised form 18 July 2022; Accepted 13 August 2022

2452-199X/© 2022 The Authors. Publishing services by Elsevier B.V. on behalf of KeAi Communications Co. Ltd. This is an open access article under the CC BY-NC-ND license (<http://creativecommons.org/licenses/by-nc-nd/4.0/>).

12,13]. Furthermore, thanks to their advantages in controllability, sustainability, and reversibility in response to temperature, thermoresponsive polymers are highly suitable for tissue engineering, regenerative medicine, and tumor diagnosis and treatment [14–22]. For example, the temperature responsiveness of these polymers was reported to synergize tumor hyperthermia therapy with chemotherapy [23,24]. From this, we found that the temperature-dependent changes of these polymers can provide new ideas for reacting to the temperature change. Therefore, the flexible response to the temperature change of the tissue is expected to become a breakthrough to address this issue.

The risk of arterial vasospasm persists after surgery. And the pathogenesis of postoperative arterial vasospasm is complicated at which point the continuous influx of extracellular calcium into the cell is the key factor. Therefore, continuous and dynamic extravascular microenvironment regulation which targets extracellular calcium influx and holds sensitivity to temperature change can be effective to manage postoperative vasospasm. Due to the small diameter of the blood vessels in microsurgery, blood flow can be blocked even by slight stimulation such as pulling and squeezing [25]. In addition, the tissues that can be used for transplantation and reconstruction are various such as skin and muscle [26,27]. For the huge different structures of these tissues, the complexity of biomaterial application is further increased. Therefore, implanting temperature-responsive materials, which can regulate the extravascular microenvironment in response to the drop in temperature by inhibiting calcium influx to alleviate tissue injury, into perivascular tissue with a precise and minimally invasive approach may become an ideal strategy for post-microsurgery management of vasospasm.

Among them, thermosensitive hydrogel based on poly (ethylene glycol) (PEG)/poly (lactic-co-glycolic acid) (PLGA) holds good biocompatibility, injectability, and extremely high drug loading rate [28]. It can be used as an *in situ* reservoir to release a therapeutic medium for a long time, and it is widely used to manage chronic diseases such as tumors and diabetes that require a stable therapeutic drug concentration [28,29]. When injected into the body, the sol–gel transition that can be achieved under the trigger of body temperature allows it to fill the lesion space regardless of its irregularity. In addition, by tuning the monomer ratio, molecular weight, molecular weight distribution, end functional groups, and copolymer concentration, the phase transition temperature can be precisely adjusted at 4–60 °C [30–35]. However, current research mainly exploits its sol–gel transition ability triggered at body temperature, and few people have exploited the reverse gel–sol transition property triggered by low temperature [36, 37]. We note that this reversible temperature-shifting property may be of unique value in vasospasm-related temperature-altered diseases. When the gel–sol phase transition temperature of the thermosensitive hydrogel is adjusted to be at the critical temperature after the occurrence of severe arterial compromise, that is, about 3 °C lower than the normal tissue temperature [5,38], this hydrogel system can provide timely detection and protection of transplanted tissue by releasing the therapeutic agents such as drugs or cells in response to the dropped temperature.

Herein, to match the therapeutic needs after microsurgery, the reversible thermosensitive (RTS) hydrogel system that can be flexibly injected into the skin, muscle, and other tissues was designed to exert both forward *in situ* gelation property and reverse transition for continuous and dynamic regulation of extravascular microenvironment targeting calcium influx to inhibit postoperative arterial vasospasm. The normal tissue temperature triggered a positive transition of hydrogel solution to a gel state and became a local sustained-release drug reservoir around the arteries to prevent the occurrence of vasospasm. The gel state hydrogel reversely transitions to a sol state in response to the drop in temperature caused by vasospasm, causing the rapid release of the drug to alleviate tissue injury. Based on the above theory, the intelligent hydrogel based on poly ( $D, L$ -lactic-glycolic acid)-poly (ethylene glycol)-poly ( $D, L$ -lactic-glycolic acid) (PELGA) was constructed and applied to the skin flap transplantation model. First, the monomer ratio and

concentration were adjusted to manipulate the phase transition temperature of the PELGA triblock polymer loaded with verapamil hydrochloride (Vera). The phase transition temperature was set to the critical temperature after vasospasm induced severe arterial compromise. Then the RTS hydrogel system Vera@RTS-Gel that can respond to the drop in temperature was engineered. The effects of Vera@RTS-Gel on extracellular calcium influx and vasoconstriction were evaluated *in vitro* from both the cellular and tissue levels. A rat transverse rectus abdominis skin flap model was established for *in vivo* experiments, in which microsurgery with and without postoperative severe vascular compromise and significant temperature change were both simulated to assess the efficacy of Vera@RTS-Gel on vasospasm and tissue survival. All the results proved that this RTS hydrogel system provided a new option for diseases that require timely detection and continuous management of the extravascular microenvironment (Scheme 1).

## 2. Materials and methods

### 2.1. Materials

PEG with the molecular weight (MW) of 1500,  $D, L$ -Lactide (LA), Glycolide (GA), stannous 2-ethyl-hexanoate, Vera, and phenylephrine hydrochloride (PE) were purchased from Sigma-Aldrich (USA). Sulfo-Cy5.5 NHS ester was purchased from Xi'an Qiyue Biology Co. Ltd (China). Live/dead Staining Kit, CCK-8 reagent, and Fluo-4 AM probe were acquired from Beyotime Biotechnology Company (China). Kits for biochemical tests were purchased from Nanjing Jiancheng Bioengineering Institute. Gibco, USA, provided Fetal bovine serum (FBS). Dulbecco's Modified Eagle's Medium (DMEM) was purchased from Hyclone (USA).

### 2.2. Experimental cells and animals

A7r5 cells were obtained from Cell Bank/Stem Cell Bank, Chinese Academy of Sciences. Human umbilical vein endothelial cells (HUVECs) were provided by Lonetics (USA). All cells were grown in DMEM with 10% FBS and 1% antibiotic solution in a constant temperature incubator with 5% CO<sub>2</sub>. C57BL/6 (C57) mice and Sprague Dawley (SD) rats were purchased from Shanghai Jiesijie Laboratory Animal Co. Ltd.

### 2.3. Synthesis of PELGA triblock polymer

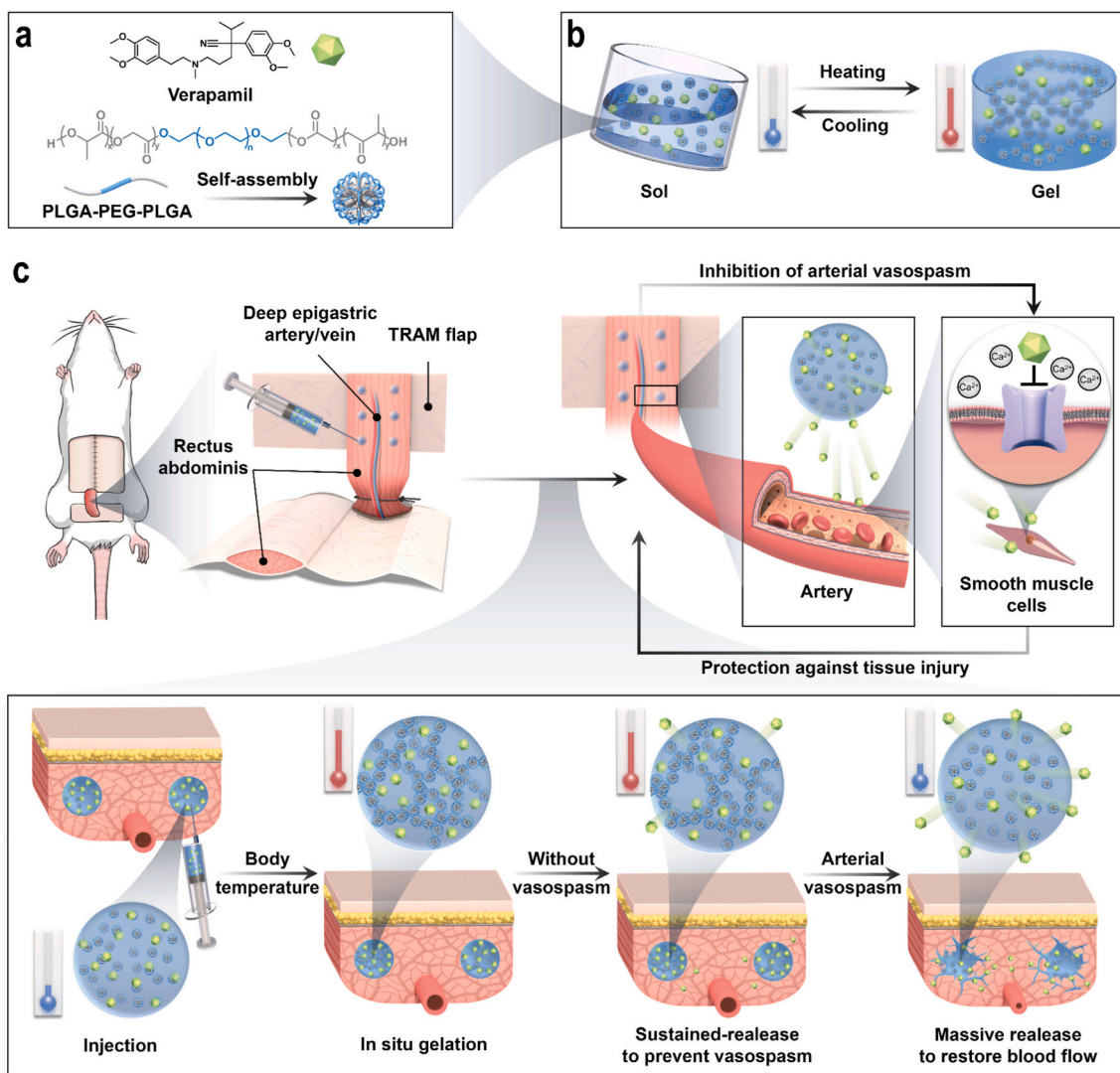
The PELGA triblock polymer was synthesized as described elsewhere [29]. Ring-opening copolymerization of GA and LA was performed with stannous octoate as catalyst and dihydroxy PEG with the MW of 1500 as a macroinitiator. 20 g of PEG was added to the three-necked flask under vacuum at the temperature of 150 °C. After 3 h, the flask was cooled to room temperature. Then GA and LA monomers were added. Argon was changed three times for the elimination of the residual moisture. After adding stannous octoate, the reaction temperature was set at 150 °C for 12 h in argon atmosphere. 80 °C water was used to rinse the crude products at least three times and the residual water was removed by lyophilization.

### 2.4. Preparation of Vera@RTS-Gel

The PELGA polymers (25 wt%) were dissolved in water at 4 °C, then Vera was dissolved in the polymer aqueous solution with concentrations of 1, 2, or 4 mg ml<sup>-1</sup>. Magnetic stirring was used to ensure complete dissolution [29].

### 2.5. <sup>1</sup>H NMR spectrum measurement

The chemical structures and compositions were acquired through the 400 MHz spectrometer (Bruker, AVANCE III HD) using CDCl<sub>3</sub> as the solvent at the temperature of 25 °C. Chemical shifts were presented in



**Scheme 1.** Schematic illustration of the RTS hydrogel to inhibit calcium influx and vasospasm. a) The fabrication of the RTS hydrogel system. b) The reversible gel–sol transition property of RTS hydrogel. c) RTS hydrogel can alleviate tissue injury with the burst release and diffusion of the drug caused by rapid reverse transitions to the sol state in response to the drop in temperature due to arterial vasospasm.

ppm with tetramethylsilane as the internal standard [29].

## 2.6. Sol–gel and gel–sol transition measurement

The tube inversion method was used to measure the transition temperature of the PELGA aqueous solution. First, the solution was dropped into the vial. Then the vial was put in a low-temperature water bath. After increasing the temperature, the vial was kept in water for 10 min and then turned upside down. If there was no flow along the wall within 30s, it was identified as a gel and the initial temperature was determined as  $T_{gel}$ . As the temperature increased, the gel became suspension, and the initial temperature was determined to be  $T_{sol}$  (suspension) [7]. By investigating a range of PELGA polymer concentrations at different temperatures, the state diagram of polymer aqueous solution was determined [29].

## 2.7. The hydrodynamic diameters, $\zeta$ potentials measurement and transmission electron microscopy (TEM) analysis

In the aqueous solution of PELGA (25 wt%) with or without different concentrations of Vera, they were measured by a DLS apparatus (Zetasizer Nano ZS90, Malvern) at the temperature of 25 °C after dialysis [39,

40]. The scattering angle was set at 90°. The morphology of PELGA (25 wt%) with or without Vera (4 mg ml<sup>-1</sup>) was observed by transmission electron microscopy (Tecnai G2, Thermofisher).

## 2.8. Rheologic behavior analysis

A strain-controlled rheometer (Kinexus, Malvern) was used to measure the transition of the aqueous solutions of the polymers with or without Vera. The collection of the viscosity ( $\eta$ ), storage modulus ( $G'$ ), and loss modulus ( $G''$ ) were acquired at a gap of 0.03 mm, a rate of 0.5 °C min<sup>-1</sup>, and a frequency of 10 rad s<sup>-1</sup> [29].

## 2.9. In vitro release studies

Release behavior of three groups of 25 wt% PELGA polymers containing different concentrations of Vera (1, 2, 4 mg ml<sup>-1</sup>) were detected *in vitro* at 37 °C. First, 0.5 g of the polymer solution was dropped into the glass tube. 5 ml PBS buffer at 37 °C was added to each tube which was balanced in a water bath for 15 min at 37 °C. At the same time every day, take out the buffer for measurement and refill it in the same way. Then the concentration of Vera in PBS was detected by high-performance liquid chromatography (HPLC) [41]. The optimum detection

wavelength of the UV detector was set at 278 nm.

### 2.10. Temperature responsiveness tests

*In vitro*, the process of injecting hydrogels dissolved with water-soluble pigments into different temperatures of water was observed continuously. *In vivo*, after loading Sulfo-Cy5.5 NHS ester, a water-soluble fluorescent molecule, the RTS hydrogel was injected into the tissue of the flaps with temperature change. The distribution of fluorescent molecules was observed by the *in vivo* fluorescence image analysis system (PerkinElmer, USA).

### 2.11. Biocompatibility evaluation

A7r5 cells and HUVEC cells were inoculated into 24 well plates and 96 well plates respectively for 12 h, and then culture medium containing different concentrations (0, 1, 5, 10, 50, 100, 500, 1000  $\mu\text{g ml}^{-1}$ ) of PELGA triblock polymer or Vera@RTS-Gel replaced the original culture medium. After 24 h of culture, live/dead staining and CCK-8 experiment were carried out [42]. Cultured cells were treated with a live/dead cell staining Kit, and they were examined with a fluorescence microscope (PCOM, Nikon, Japan). In the CCK-8 experiment, the absorption was measured with a flex station 3 microplate reader (molecular devices, Japan) at 450 nm after 1 h of treatment. Aqueous solutions of Vera@RTS-Gel were prepared and then subcutaneously injected into the backs of rats using a 1 ml syringe. The injection volume of the hydrogel was 0.3 ml per rat. After 1, 3, or 7 days, rats were euthanized with gas, and tissue samples were taken for histological analysis.

### 2.12. Measurement of calcium influx

A7r5 cells were inoculated into 12 well plates and loaded with fluo-4 AM [43,44]. For each group, the cells were treated respectively with Krebs-Henseleit solution with or without Vera or the release solution of the Gel or Vera@RTS-Gel in Krebs-Henseleit solution on the first day or the fourth day. The concentration for the Vera group was chosen based on the average concentration of the release solution from 7 days (82  $\mu\text{M}$ ). Then the cells were incubated with calcium-free buffer. Calcium influx was triggered by adding 2.5 mM  $\text{CaCl}_2$ , and fluorimetric measurements were recorded continuously by the fluorescence microscope (PCOM, Nikon, Japan) [45]. Then the fluorescence intensity of cells was measured by image J. Changes in fluorescence intensity were indicated by comparing the maximal fluorescence intensity ( $F_{\text{max}}$ ) to that measured at the starting point ( $F_0$ ).

### 2.13. Preparation of arterial rings and measurement of isometric tension

C57 mice were sacrificed by neck dislocation and then the main mesenteric arteries were isolated and placed into cold oxygenated Krebs solution. The arteries were cut into ring segments after clearing the connective tissues. Then the arterial rings were mounted into the 620 M Microvascular Tension Measurement System (DMT, Denmark) as previously described [43,44]. After treatment with 60 mM KCl to obtain stable basal tension, the organ chamber was washed and then refilled with 5 ml Krebs solution with or without Vera, or the release solution of the Gel or Vera@RTS-Gel in Krebs solution on the first day or the fourth day for 5 min respectively. Then PE was added to form a concentration gradient, and the real-time tension changes of the arterial rings were recorded with the Power Lab Biological Signal Collection System (AD Instruments, Australia).

Contraction = (Maximal tension by PE)/(Basal tension by 60 mM KCl).

### 2.14. Animal model of the free TRAM flaps

SD rats were randomly divided into the non-ischemic or the ischemic

treatment group. Then rats in the first group were divided into the Control, Gel, Vera, and Vera@RTS-Gel groups ( $n=3$ ), and those in the latter group were divided into the Sham, Control, Gel, Vera, and Vera@RTS-Gel groups ( $n=3$ ). The steps of the operation were followed by previous studies [46–48]. According to the general method, 6 cm \* 3 cm skin tissue and the right side of the connected rectus abdominis muscle under the costal arch were lifted as the free TRAM flaps. The flap was lifted and the blood flow was achieved solely through the deep inferior epigastric vessels. The anastomosis and recanalization of blood vessels are simulated by clamping the pedicle of blood supply vessels. After restoring blood flow, for the Gel and Vera@RTS-Gel groups, the peripheral vascular muscle tissues were injected with the hydrogel solution in a multisite manner with the total volume of 0.05 ml per rat. Before the flap was sutured in situ, a sterile silicone sheet was placed under the elevated flap to prevent revascularisation. The Vera group received an intraperitoneal injection of normal saline solution with Vera once a day after surgery (0.1 ml, 0.25  $\text{mg ml}^{-1}$ ). The drug dosage was decided based on previous studies [49,50]. Routine feeding and care in the clinic were performed after surgery. In the ischemic treatment group, the flap was lifted on the first day after surgery, and an atraumatic microclamp was applied in the vascular pedicle except for the Sham group. Thermal insulation measures were used to avoid the effect of the body temperature on the skin flaps. For the Vera group, a topical injection of normal saline solution with Vera was performed immediately after ischemic treatment (0.3 ml, 0.25  $\text{mg ml}^{-1}$ ). After 4 h, the blood perfusion of the flap was restored. After 24 h of reperfusion, the rats were euthanized with gas and the flap was harvested for further study.

### 2.15. The vascular ultrasonic Doppler detection

On day 1 and day 4 after surgery, vascular ultrasonic Doppler detection (the VEVO lazr-x multimodal imaging platform, Fujifilm VisualSonics, Japan) was used to detect the blood flow of the deep inferior epigastric artery. Firstly, the position of the distal end of the deep abdominal artery was located to obtain a stable peak systolic flow velocity. Then, ice bags were used for hypothermic stimulation at the proximal end, and records were made after the flow velocity was stable [51]. Rats in the Vera group repeated the above tests before and after the intraperitoneal injection. All the rats were exposed to anesthesia (isoflurane) in this experiment.

### 2.16. Biochemical examination

24 h after the blood flow was restored, the distal tissue samples which were accurately weighed were made into tissue homogenate for the detection of malondialdehyde (MDA) levels, reduced glutathione (GSH) levels, superoxide dismutase (SOD) activity, and neutrophil myeloperoxidase (MPO) activity according to previous studies and the instructions of kits [52,53].

### 2.17. Macroscopical evaluation and histological analysis

In the non-ischemic treatment group, on day 7 after surgery, all the rats were anesthetized with gas, and the flap was photographed. Then the percentage of necrosis area was quantitatively evaluated by image J. Skin samples were obtained from the junction of necrosis and survival of the flap, and muscle samples were obtained from the muscular part of the flap for morphological analysis [54]. In the ischemic treatment group, 24 h after the blood flow was restored, the muscle and skin tissue samples of the flaps were taken for morphological analysis. Rats for biocompatibility evaluation were euthanized with gas and the skin samples of the injection regions were taken for histological analysis. All samples requiring morphological analysis were fixed in 4% neutral formalin for 24 h. The tissue sections were stained with Hematoxylin-eosin (HE) staining and Masson trichrome staining after

paraffin embedding. The samples were observed by the bright-field microscope.

### 2.18. Statistical analysis

All data were displayed as mean  $\pm$  standard deviation (SD). Statistical analysis was performed using GraphPad Prism software. The differences between groups were evaluated using one-way analysis of variance (ANOVA) and Tukey multiple comparison.  $p < 0.05$  was considered statistically significant, while ns meant no statistical difference.

## 3. Results and discussion

### 3.1. Preparation and characterization of Vera@RTS-Gel

In this study, to achieve the responsiveness to temperature change and release drugs to exert therapeutic effects, the drug loading function of PELGA triblock polymer was an important basis. First, the synthesis of PELGA triblock polymers was carried out by ring-opening polymerization of La and GA using PEG as initiator and stannous octoate as the catalyst according to the method of previous studies [29]. Then NMR hydrogen spectroscopy was used for the analysis of the chemical structure. Fig. 1a shows the  $^1\text{H}$  NMR spectra and chemical structures of the triblock polymer. The number-average MW,  $M_n$ , was obtained with peak integrals at 4.80 ( $-\text{COCH}_2\text{O}-$ ), 3.65 ( $-\text{CH}_2\text{CH}_2\text{O}-$ ), and 1.55 ( $-\text{COCH}(\text{CH}_3)$ )

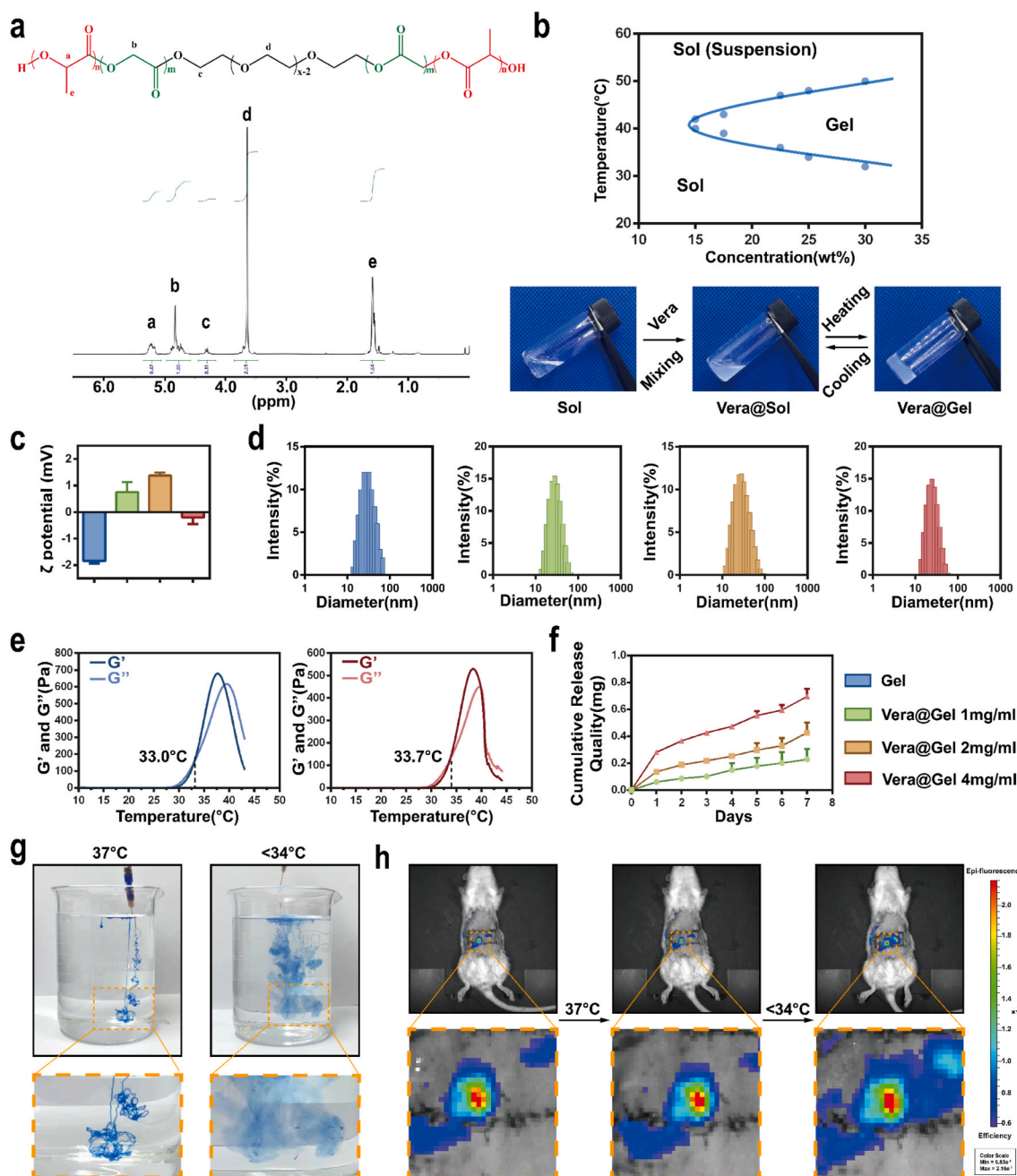


**Fig. 1.** Characterization of PELGA polymers before and after loading Vera. a)  $^1\text{H}$  NMR results of the PELGA polymers. b) Phase diagram and transition property of the PELGA polymers. c)  $\zeta$  potential measurement, d) micelle size distribution and e) changes of  $G'$  and  $G''$  of the PELGA polymers with or without Vera. f) Cumulative release curve of PELGA polymers containing different concentrations of Vera ( $n = 3$ ). Temperature responsiveness of the RTS hydrogel system g) *in vitro* and h) *in vivo*.

O-) ppm. As shown in Fig. 1b, the aqueous solution of triblock polymer could form a semisolid gel under the triggering of temperature, and upon recovery of low temperature, it could quickly transform into a flowing sol state. And below or above the sol–gel transition temperature ( $T_{gel}$ ), the solution was presented as two different morphologies. And the  $T_{gel}$  of the polymer system can be adjusted between 32 and 50 °C depending on the polymer concentration as well as the ratio of monomers [30–32]. In this study, the adjustment of the system was performed based on these variables. For the need for treatment of vasospasm after microsurgical free flap transplantation, Vera, a calcium antagonist, was selected as the therapeutic medium [50,55]. Vera-loaded PELGA triblock polymer hydrogel was prepared by homogeneous mixing of Vera and PELGA aqueous solution at 4 °C. As shown in Fig. 1c, we characterized the surface of polymeric micelles before and after the addition of Vera by  $\zeta$  potential change, this change illustrated the recombination between polymer and Vera occurred through the way of electrostatic interaction. In Fig. 1d, dynamic light scattering (DLS) particle size analysis indicated that amphiphilic polymers could self-assemble in an aqueous system to form micelles with particle size around 35 nm while adding Vera wouldn't affect the structure and size of micelles. Transmission electron microscopy (TEM) analysis also showed the similar morphology of micelles before and after loading Vera with the particle size consistent with the DLS measurements (Fig. S3).

To respond to the temperature change resulting from vasospasm, the RST hydrogel first needs to have an appropriate transition temperature that can be easily tuned according to different circumstances. Taking the microsurgical free flap transplantation as an example, clinical experience suggests that after the occurrence of severe arterial compromise, the temperature decreases by about 3 °C, so the transition temperature was set at about 34 °C. Considering the possible effects caused by the drug-loading, the changes in properties such as  $T_{gel}$  after the addition of Vera needed to be examined. As shown in Fig. 1e, a strain-controlled rheometer was used for the investigation of the transition property of the aqueous polymer solutions over temperature. With the increase in temperature, the storage modulus ( $G'$ ) gradually exceeded the loss modulus ( $G''$ ), and the viscosity of the polymer solution increased abruptly, indicating in situ gelation forming an osmotic micelle network through micelle aggregation. In general, the temperature where  $G'$  equals  $G''$  is regarded as the  $T_{gel}$ . Upon examination, a slight increase in  $T_{gel}$  occurred after loading Vera. By validating the transitions of different formulations, we found that when Vera at a concentration of 4 mg ml<sup>-1</sup> was loaded into the triblock polymer solution with a concentration of 25 wt%,  $T_{gel}$  could be located around 34 °C. It firstly guaranteed the injectability of the system as well as the ability of in situ gelation and, most importantly, fulfilling the demand of responsiveness to the temperature change due to vasospasm.

It's also very important for RTS hydrogel to have proper slow-release behaviors because the therapeutic effect against vasospasm triggered by temperature change requires sustained maintenance of the drug content for a period after surgery. *In vitro*, the study of the release behavior of PELGA hydrogels loaded with different concentrations of Vera was performed over 7 days. PBS solution was added after transitioning to a gel state, and the concentration of release solution was accurately detected by HPLC at the maximum absorption wavelength. The plotted release profiles suggested that an effective slow-release was achieved within 7 days (Fig. 1f). For the first day, the hydrogel systems containing various amounts of Vera released an average of 24.19%, 27.21%, and 28.17% of the total amount. Respectively, during the second to seventh days, a relatively uniform release occurred every day, and the release behaviors at different concentrations were not significantly different. So, they could all be regarded as effective sustained delivery systems. Based on the above results, the hydrogel prepared by loading Vera (4 mg ml<sup>-1</sup>) into the triblock polymer solution (25 wt%) was selected for subsequent study.

Subsequently, for the Vera-loaded “reversible thermosensitive” hydrogel (Vera@RTS-Gel) as prepared, we examined the temperature-

responsive capabilities *in vitro* and *in vivo*. As shown in Fig. 1g, when injected into water at different temperatures, the hydrogel exhibited different states immediately upon exposure to the water surface. When the temperature was lower, the pigments dissolved rapidly into the surrounding water from the hydrogel of a sol state. A gel state was maintained when the temperature was higher, and the pigments were concomitantly maintained therein. In Fig. 1h, after injection of RTS hydrogel loaded with water-soluble fluorescent molecules into the free flap tissue, the effect on drug diffusion was observed with *in vivo* fluorescence imaging system at different temperatures of the tissue. The results illustrated that the RTS hydrogel can maintain a stable gel state at normal body temperature while undergoing a reverse gel–sol transition and rapid drug release at low temperature. These results showed that the state and associated release behaviors of RTS hydrogel could rapidly respond to temperature change. It provided a foundation for dynamically regulating the extravascular microenvironment by exerting in situ gelation after injection in combination with exerting therapeutic effects to respond to temperature change caused by vasospasm.

### 3.2. Biocompatibility of PELGA polymers and Vera@RTS-Gel

PELGA triblock polymers have been proven to have good biocompatibility in a variety of disease models, and in this experiment, rat smooth muscle cell line (A7R5s), as well as human umbilical vein endothelial cells (HUVECs), were used for revalidation for that. We evaluated the effect of PELGA triblock polymers on cell survival by cell live/dead staining assay and CCK-8 assay. As shown in Fig. 2a–b and Fig. S1, cells were cultured with cell culture media that dissolved different concentrations of PELGA polymers, and both cells could maintain the vast majority of survival even at higher concentrations. The CCK-8 experiment shown in Fig. 2c also verified this conclusion. With the concentration increases, there was no significant difference compared with the control group. As for the Vera@RTS-Gel, its biocompatibility was tested the same way (Fig. S4). Aqueous solutions of Vera@RTS-Gel were injected subcutaneously in rats and histological analysis was performed on day 1, 3, or 7 after implantation. As shown in Fig. S5, the local inflammatory responses were modest. The results illustrated the good biocompatibility of PELGA triblock polymers and Vera@RTS-Gel which provided an important basis for the application in microsurgery.

### 3.3. *In vitro* effects of inhibiting extracellular calcium influx and vasospasm

As a key factor in the contraction of the smooth muscle, the rise of Ca<sup>2+</sup> concentration within vascular smooth muscle cells (VSMCs) has a close relationship with the excitation-contraction coupling. The essence of vasospasm is the continuous spasm contraction of vascular smooth muscle locally, at which point the increase of Ca<sup>2+</sup> concentration relies on the continuous influx of extracellular Ca<sup>2+</sup> into the cell [55,56]. Being able to block Ca<sup>2+</sup> influx would target the key factors against vasospasm. To verify this effect of the RTS hydrogel, the calcium indicator fluo-4 AM molecular probes were used to visually reflect the Ca<sup>2+</sup> concentration in A7R5 cells. Upon stimulation by elevated extracellular Ca<sup>2+</sup> concentrations, it was possible to visualize the rise in intracellular Ca<sup>2+</sup> concentrations as a result of the influx of Ca<sup>2+</sup> with a fluorescence microscope (Fig. 3b). The strongest fluorescence intensity after stimulation was subsequently used for comparison with the initial one. Compared with the rises in the Control group and the Gel group which were more than 3-fold, those in the Vera@RTS-Gel group were significantly suppressed and were comparable to the Vera group (Fig. 3a and c). The above results verified that at the cellular level, the RTS hydrogel played a role in inhibiting vasospasm by restricting the extracellular Ca<sup>2+</sup> influx.

With the microvascular tension measurement system and stimulation induced by PE, tension changes in microvascular constriction could be

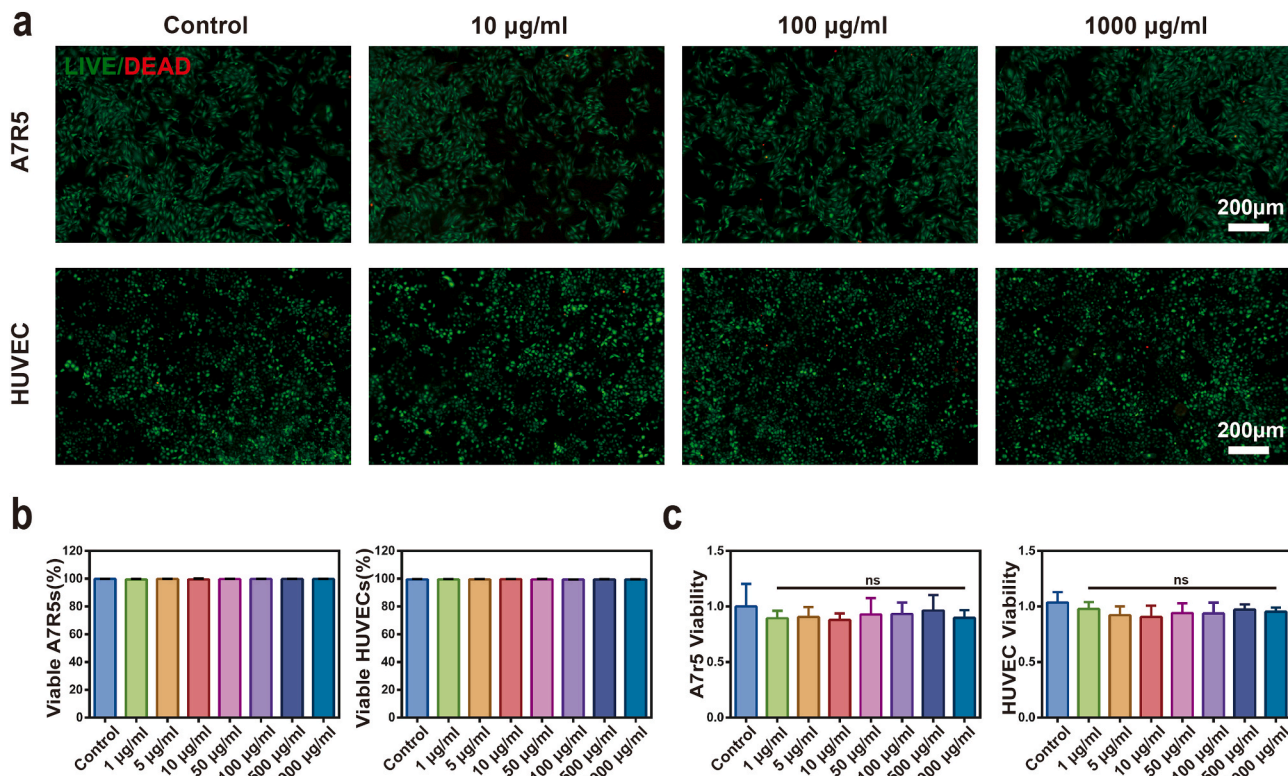


Fig. 2. Biocompatibility of PELGA polymers. a) The live/dead staining of A7r5 and HUVEC cells and b) the proportion of living cells after 24 h incubation with different concentrations of polymer in the culture medium ( $n = 4$ ). c) The CCK-8 test results of A7r5 and HUVEC cytotoxicity after 24 h incubation with different concentrations of polymer in the culture medium ( $n = 4$ ). (ns: not significant).

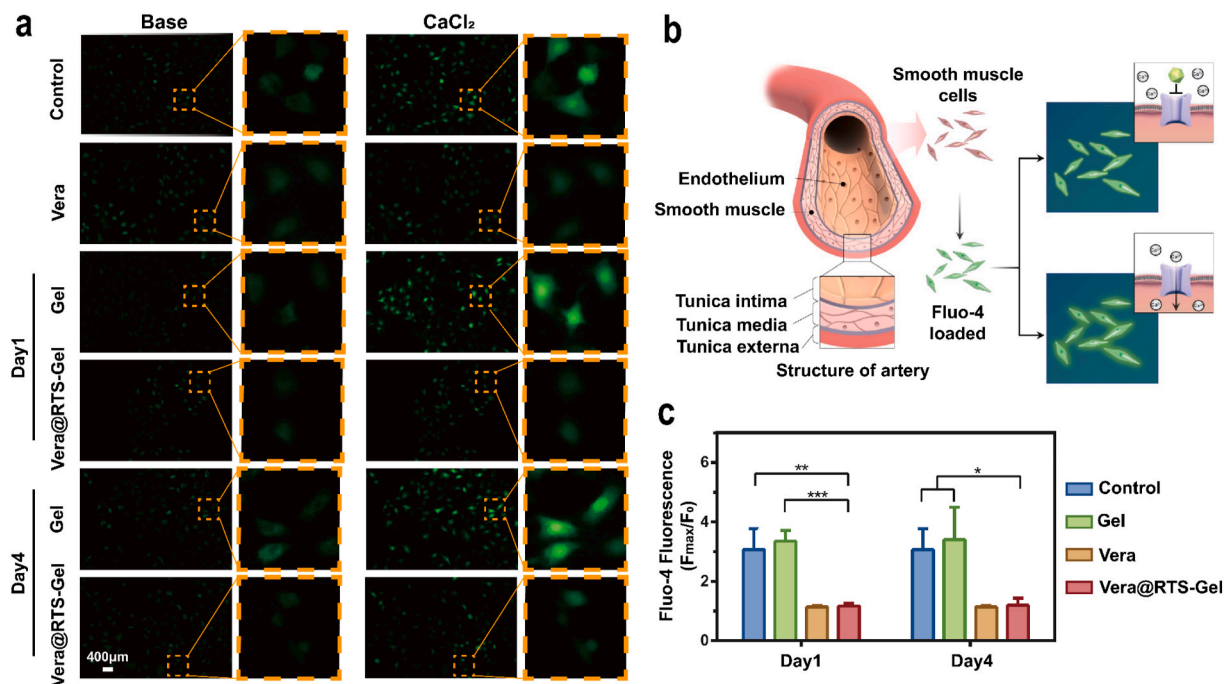
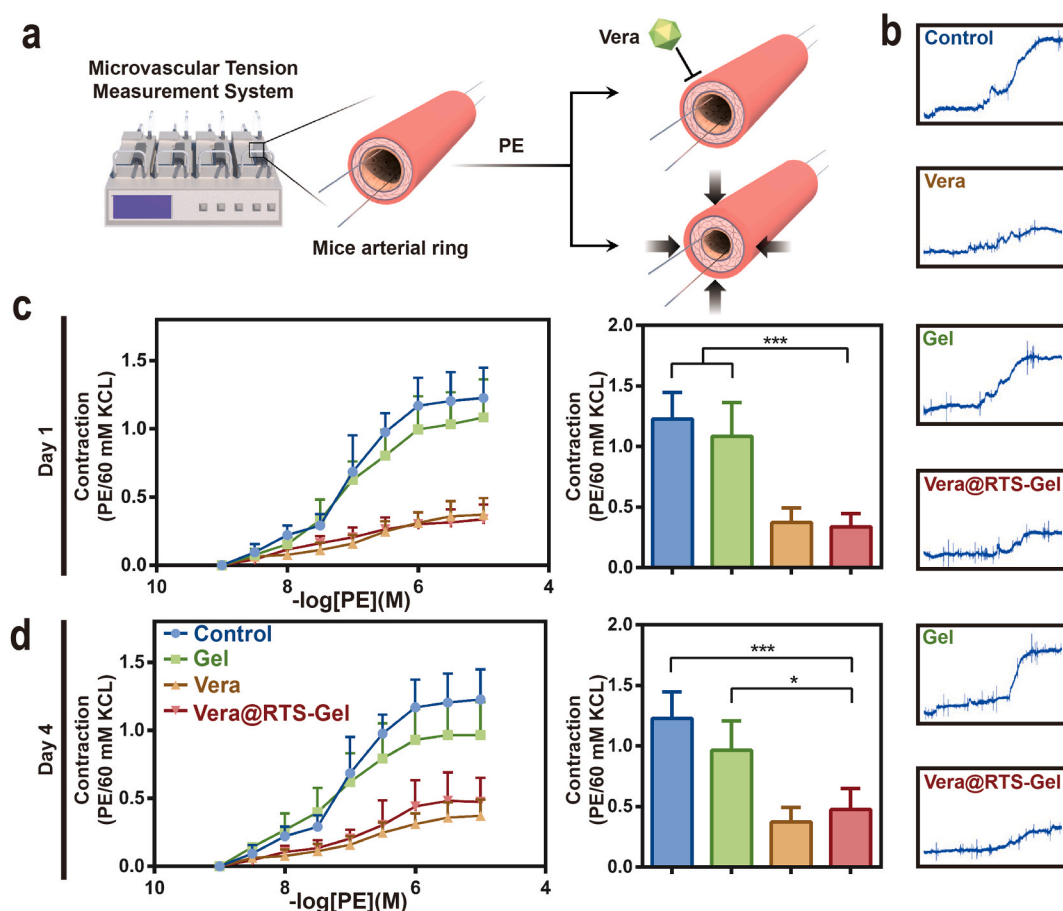


Fig. 3. RTS hydrogel inhibits the extracellular calcium influx *in vitro*. a) Representative images. b) The schematic of the calcium influx test in A7r5 cells. c) Summarized graph of maximal change in fluorescence intensity in A7r5 cells as measured by the calcium indicator fluo-4 ( $n = 3$ ). ( $*p < 0.05$ ,  $**p < 0.01$ ,  $***p < 0.005$ ).

steadily induced and accurately displayed [57,58]. Based on this, we examined the effects to inhibit vasospasm at the level of vascular tissue. After incubation with either the release solution of the PELGA hydrogel or Vera@RTS-Gel on day 1 or 4, the addition of PE caused the

concentration-dependent responses of arterial rings, compared with other groups (Fig. 4a). Real-time tension changes were obtained with the signal collection system and assessed by comparison with the basal tension induced by 60 mM KCl. Fig. 4b-d demonstrated that the



**Fig. 4.** RTS hydrogel inhibits vasospasm *in vitro*. a) The schematic of tension measurements of the PE-induced contraction of the arterial rings. b) Representative images of the PE-induced tension changes. The contraction curves and summarized graph of maximal contraction change of c) day 1 and d) day 4 ( $n = 4$ ). (\* $p < 0.05$ , \*\*\* $p < 0.005$ ).

PE-induced contraction curves in the Vera@RTS-Gel group showed a rightward shift. As shown in Fig. 4c and d, the maximal contraction in the Vera@RTS-Gel group ( $0.3372 \pm 0.1085$  on day1,  $0.4754 \pm 0.1741$  on day4) was significantly lower than that in the Control group ( $1.227 \pm 0.2210$  and  $0.9656 \pm 0.2411$  on day4) and comparable to that in the Vera group ( $0.3724 \pm 0.1195$ ).

Above, from the level of cells and tissues, both the initiating factor with calcium influx and the final manifestation of vascular tone was examined. We verified the inhibition effect of RTS hydrogel which provided the basis for its use to regulate the extravascular microenvironment by inhibiting calcium influx and vasospasm to promote tissue survival *in vivo*.

### 3.4. *In vivo* effect of inhibiting vasospasm and promoting flap survival

To investigate the effect of the RST hydrogel *in vivo*, we selected the animal model of the free rectus abdominis transverse (TRAM) flap with a well-defined vascular pedicle for blood supply. Clinically, for this class of free flaps, the most critical factor for survival lies in the blood supply of the vessels, and thus their tissue survival will reflect the results of postoperative vasospasm management. To exclude the instability of the vascular anastomosis operation, we took the clamping and unclamping using microclamps to simulate this process. Subsequently, after the recovery of blood flow, a syringe was used to inject the hydrogel solution in a multisite manner around the arteries to avoid compression on them. Upon the stimulation of body temperature, the hydrogel after injection underwent an *in situ* sol-gel transition due to micellar aggregation to

become a perivascular drug-releasing reservoir (Fig. 5a). As required in the clinical flap operations, care was taken to avoid the adverse effects of low temperature on flap survival.

The subsequent study was carried out in two aspects, which simulated the conditions with or without temperature decrease due to vascular compromise caused by arterial vasospasm. For rats not subjected to ischemic treatment, routine feeding was performed. To examine the inhibitory effect on arterial vasospasm *in vivo*, we evaluated the response of arterial vessels to local hypothermia stimulation. On day 1 and day 4 after surgery, the proximal side of the artery was stimulated using an ice bag, and the changes in systolic maximum flow velocity on the distal side were measured by real-time monitoring with an ultrasonic Doppler imaging system (Fig. 6a). The effect on blood supply after vasoconstriction was illustrated by the ratio of the velocity after stimulation to that before stimulation. The results suggested that in the Vera@RTS-Gel group, the ratio was significantly larger in comparison with those in the Control group, the Gel group, and the Vera group before treatment. The Vera group, as a representative of routine treatment, showed different performances before and after administration which exhibited the instability of local drug concentration (Fig. 6b and c). All the above results indicated that Vera@RTS-Gel, as a sustained-release reservoir of drugs, could maintain a more stable perivascular drug concentration and better play a role in regulating the extravascular microenvironment by inhibiting vasospasm for a sustained period after surgery.

In general, the survival of the flap is the most intuitive manifestation of the surgical outcome. Observation for flap survival on day 7 after surgery was chosen for clear discernment at that time [59–61]. The rate

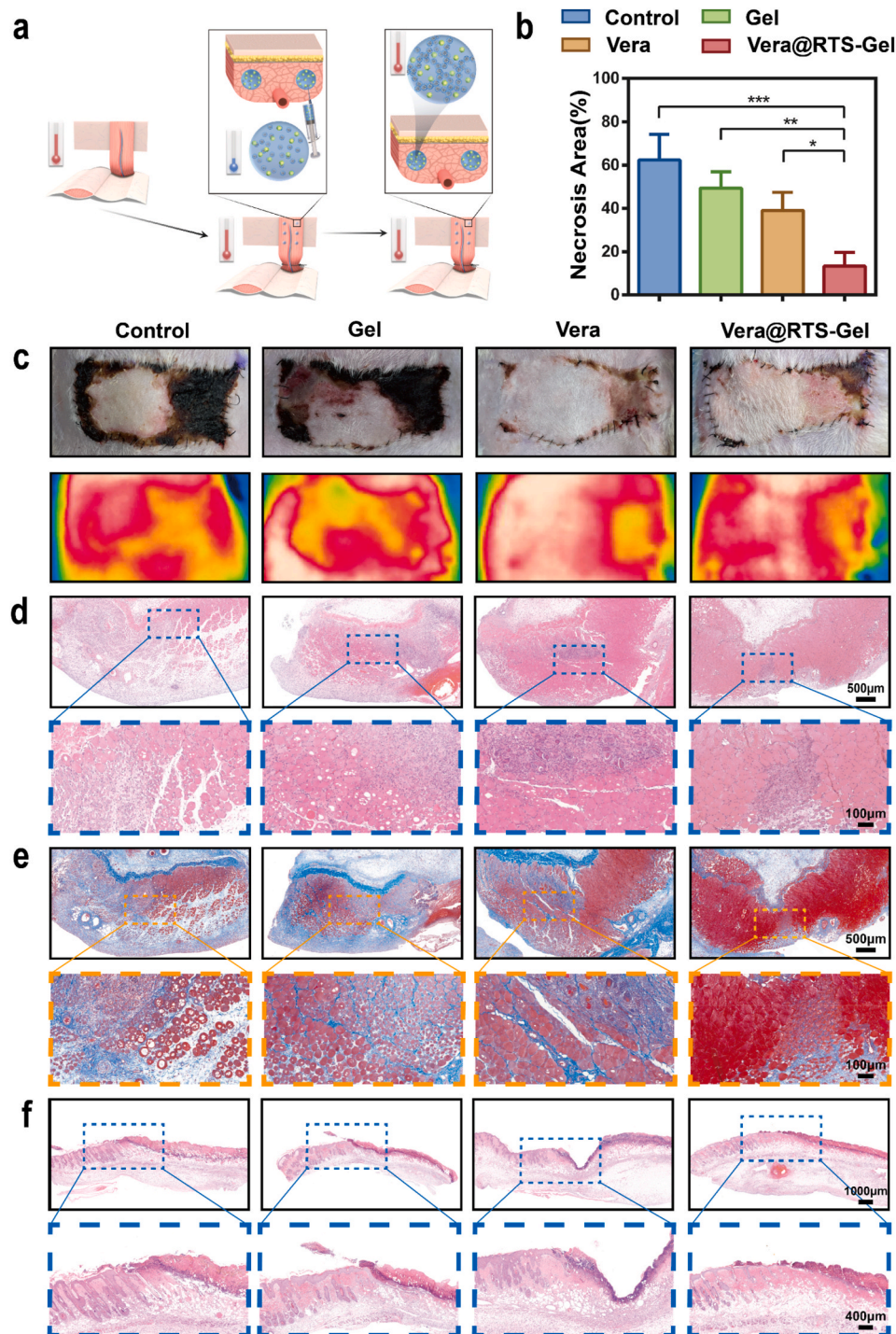


**Fig. 5.** RTS hydrogel promotes tissue survival. a) The schematic of the animal experiments. b) Flap necrosis area percentages of different groups ( $n = 3$ ). c) Skin flap appearance and thermal images of each group. d) HE and e) Masson staining of the muscle tissue. f) HE staining of the junction of the necrosis and survival area of the skin flaps. (\* $p < 0.05$ , \*\* $p < 0.01$ , \*\*\* $p < 0.005$ ).

of flap necrosis was expressed as necrotic area/total flap area  $\times 100\%$ , and the necrotic versus viable skin showed a well-defined demarcation (Fig. 5c). As shown in Fig. 5b, the average necrosis rate in the Vera@RTS-Gel group ( $13.31 \pm 6.332\%$ ) was significantly improved from those in the Control group ( $62.39 \pm 11.85\%$ ), the Gel group ( $49.42 \pm 7.537\%$ ) and the Vera group ( $39.04 \pm 8.411\%$ ). The subsequent histological observation was performed after taking samples from the muscle tissue of the flap and the skin tissue from the junction of the necrosis and survival area of the flap. In the Control group and the Gel group, HE staining and Masson staining of the muscle tissue showed a

wide range of myocyte regeneration with hyperplasia of collagen fibers due to massive destruction of normal muscle tissue, and the structure was significantly altered compared with the normal tissue, whereas in the Vera@RTS-Gel Group only small areas manifested as abnormal (Fig. 5d and e). HE staining of the skin revealed that the depth of necrosis and the degree of tissue destruction was significantly more severe in the Control group and the Gel group, whereas necrosis in the Vera@RTS-Gel group was confined to the superficial layer (Fig. 5f). From the above results, it can be speculated that the Vera@RTS-Gel system, with an effect superior to conventional treatment modalities,

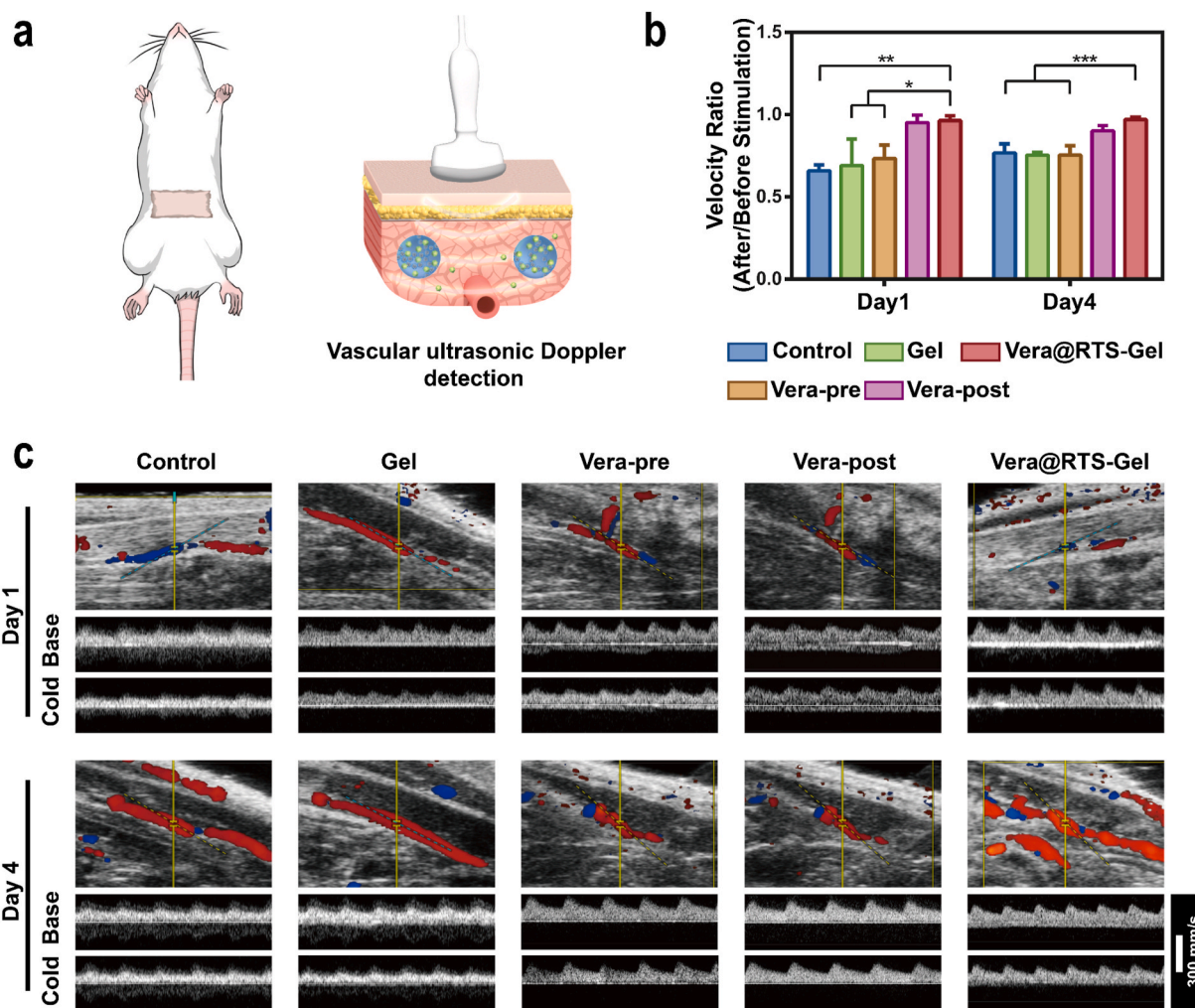


**Fig. 6.** RTS hydrogel inhibits vasospasm *in vivo*. a) The schematic of the vascular ultrasonic Doppler detection. b) Summarized graph of velocity ratio of each group ( $n = 3$ ). c) Representative images of the blood flow and the flow velocity of each group before and after the cold stimulation. ( $*p < 0.05$ ,  $**p < 0.01$ ,  $***p < 0.005$ ).

is a therapeutic modality with application potential to prevent the occurrence of postoperative arterial vasospasm and promote tissue survival.

### 3.5. *In vivo* effect of alleviating tissue injury in response to the drop in temperature

To explore whether the RTS hydrogel implanted into the tissue could rapidly respond to the drop in temperature induced by vasospasm to initiate the protective effect, we performed a simulation of ischemic treatment for the flaps on day 1 after surgery. Lifting the flaps and preventing the blood flow would cause a drop in temperature due to a lack of blood perfusion. Then the implanted RTS hydrogel could reverse to a sol state responding to the drop in temperature and release the drug in a large amount (Fig. 7a). In the Vera group, which represented the routine clinical treatment, rats were treated by topical injection of Vera immediately after ischemic treatment, which is almost impossible in clinical practice. The remaining treatment groups were the Sham group without ischemic treatment, the Control group, and the Gel group with ischemia treatment. After ischemic treatment and reperfusion, tissue samples were taken for further analysis. During this process, both the ischemia itself as well as the subsequent reperfusion process could cause cellular damage to the flap tissue. The outcome is closely related to the ischemic time [38], so in clinical practice, early administration of vasodilator drugs is to relieve vasospasm as soon as possible, restore

perfusion, and shorten the ischemic time. In addition to this, various studies have also shown that calcium antagonists have protective effects against ischemic tissue [62,63]. Tissue ischemia-reperfusion injury is mediated by oxygen free radicals. SOD and GSH are important antioxidants in the body, and the activities of SOD and the levels of GSH decrease when oxygen-free radical production is excessive [64]. MDA, one of the end products of lipid peroxidation reaction, is closely related to free radical metabolism [65,66]. MPO is a hallmark enzyme of neutrophils and directly correlates with the number of neutrophils [67,68]. So, we took the tissue distal to the flap for these biochemical analyses to reflect the degree of tissue injury. As shown in Fig. 7b–e, the degree of tissue injury in the Vera@RTS-Gel Group had obvious improvement compared with those not only in the Control group and the Gel group but also in the Vera group. This may be related to the fact that the RTS hydrogel regained the gel state after reperfusion and kept serving as the reservoir to release drug thereafter, which was consistent with the conclusion of the related research [69]. The subsequent histological analysis also showed that the necrotic degeneration degree of muscle fibers and the infiltration degree of inflammatory cells were significantly improved in muscle tissues among the groups with drug taking effects, and the structure of skin tissues was also closer to normal tissues (Fig. 7f and g). The above results illustrated that the RTS hydrogel had a protective effect against tissue injury caused by arterial vasospasm, suggesting a promising therapeutic effect by dynamically regulating the extravascular microenvironment with sensitive responsiveness to the

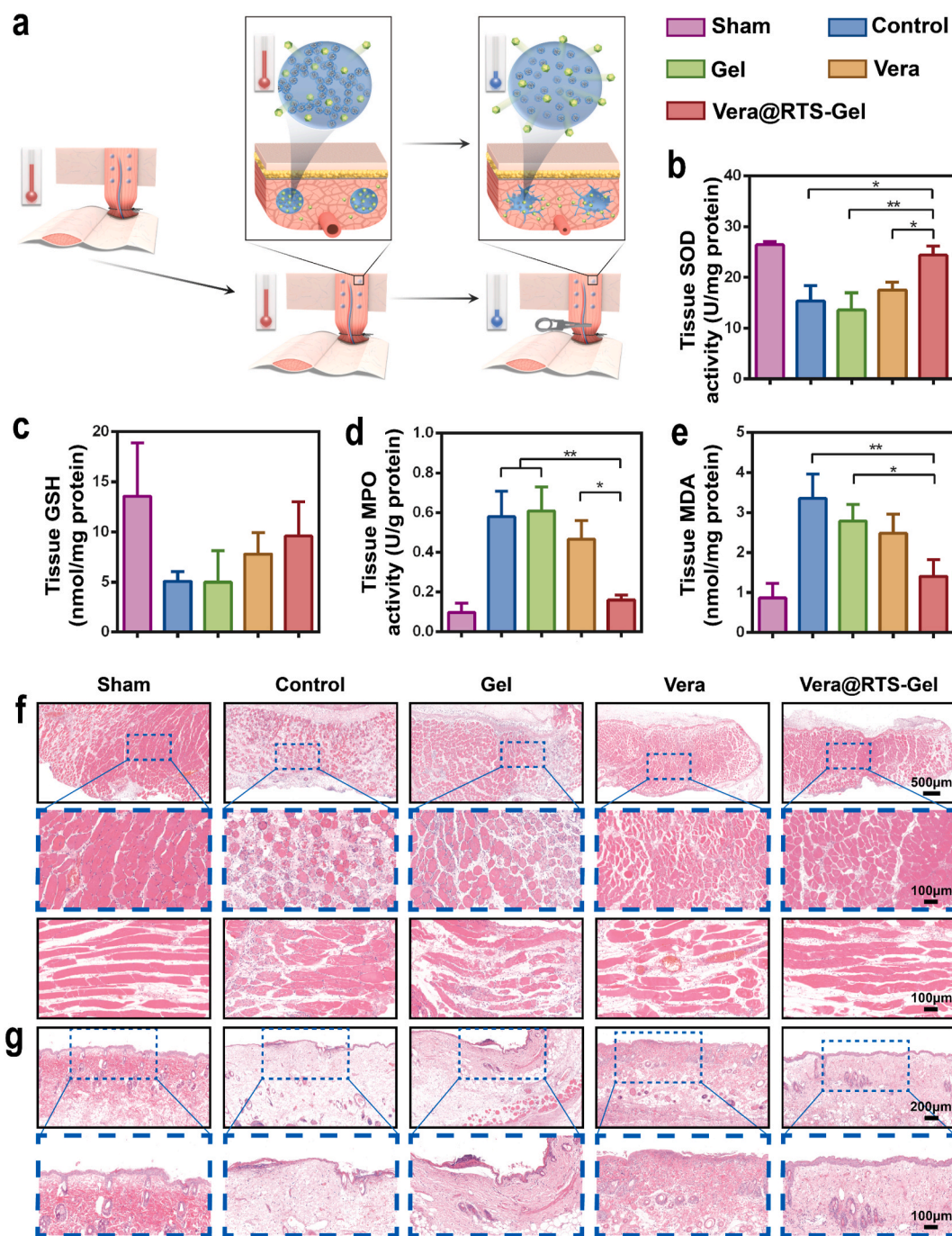


**Fig. 7.** RTS hydrogel alleviates tissue injury with the drop in temperature. a) The schematic of the animal experiments. The levels of b) SOD, c) GSH, d) MPO, and e) MDA of each group ( $n = 3$ ). f) HE staining of the muscle tissue. g) HE staining of the skin tissue. (\* $p < 0.05$ , \*\* $p < 0.01$ ).

temperature change.

It is also important to demonstrate the fate of Vera@RTS-Gel. Vera@RTS-Gel system has two fates *in vivo*. When it serves as a sustained-release reservoir to release drugs around the arteries, Vera is released by diffusion and degradation of the hydrogel to affect the local drug concentrations. As for the PELGA hydrogel, it is left in place and gradually degrades over time [70]. The degradation time of the hydrogel is longer than the release time of the drug, mainly because Vera is hydrophilic, and we need to balance the early sudden release of Vera with the long-term slow release of Vera. The PELGA hydrogel is composed of small molecular chain segments of dihydroxy PEG with the MW of 1500 and PLGA. Among them, PEG can be metabolized and excreted through the kidneys. The synthesized PLGA is connected by an ester bond, which

can be hydrolyzed into lactic acid and glycolic acid with good biocompatibility and easy excretion *in vivo* [28,70,71]. When the temperature drops caused by arterial vasospasm, the hydrogel reversely changes to the sol state, causing rapid drug release to affect the local drug concentrations around the arteries. In this case, the sol can also be discharged from the body through metabolism [28,71].

#### 4. Conclusion

Based on the need for immediate response to the drop in temperature resulting from arterial vasospasm after microsurgery, in this study, RTS hydrogel was designed and prepared based on PELGA triblock polymers. To meet the requirements of this series of diseases, it is critical to

precisely regulate the transition temperature at the critical decreased temperature. In this study, taking free flap transplantation as an example, we designed RTS hydrogel loaded with Vera to prove this concept. We demonstrated that it could exert both forward in situ gelation and reverse transition properties for the continuous and dynamic regulation of the extravascular microenvironment. After being flexibly injected into the tissues around the arteries, the RTS hydrogel converted to a gel state triggered by body temperature and became a sustained-release reservoir to reduce the incidence of vasospasm. In response to the drop in temperature caused by vasospasm, it reversely converted to a sol state to rapidly release drugs to alleviate tissue injury. From this, we can predict that RTS hydrogel, due to its flexible regulation of the transition temperature and wide applicability for loading different therapeutic mediators, holds great application potential in the monitoring and management of a range of diseases that require instant response to temperature change.

### Ethics approval and consent to participate

The animal experiments were in accordance with international ethics guidelines and the National Institutes of Health Guide, concerning the Care and Use of Laboratory Animals. The animal experiments were approved by the Ethical Committee of Shanghai Ninth People's Hospital Affiliated Shanghai Jiao Tong University School of Medicine (HKDL - 2018–141).

### CRedit authorship contribution statement

**Binfan Zhao:** Investigation, Methodology, Writing – original draft. **Yaping Zhuang:** Investigation, Methodology, Writing – review & editing. **Zhimo Liu:** Methodology, Formal analysis. **Jiayi Mao:** Formal analysis. **Shutong Qian:** Formal analysis. **QiuYu Zhao:** Validation. **Bolun Lu:** Visualization. **Xiyuan Mao:** Data curation, Software. **Liu-cheng Zhang:** Conceptualization, Methodology. **Yuguang Zhang:** Supervision, Funding acquisition. **Wenguo Cui:** Supervision, Conceptualization, Funding acquisition, Writing – review & editing. **Xiaoming Sun:** Supervision, Funding acquisition, Writing – review & editing.

### Declaration of competing interest

The authors declare no conflict of interest.

### Acknowledgements

This study was supported by the National Key Research and Development Program of China (2020YFA0908200), National Natural Science Foundation of China (81772099, 81801928 and 52103173), China Postdoctoral Science Foundation (2021M692105), Shanghai Municipal Health Commission (20204Y0354), Shanghai Municipal Key Clinical Specialty (shslczdzk00901), Young Physicians Innovation Team Project of the Ninth People's Hospital of Shanghai Jiao Tong University School of Medicine (QC201902).

### Appendix A. Supplementary data

Supplementary data to this article can be found online at <https://doi.org/10.1016/j.bioactmat.2022.08.024>.

### References

- [1] J.A. Ricci, P.G. Koolen, J. Shah, A.M. Tobias, B.T. Lee, S.J. Lin, Comparing the outcomes of different agents to treat vasospasm at microsurgical anastomosis during the papaverine shortage, *Plast. Reconstr. Surg.* 138 (3) (2016) 401e–408e, <https://doi.org/10.1097/prs.0000000000002430>.
- [2] C.M. Boutry, L. Beker, Y. Kaizawa, C. Vassos, H. Tran, A.C. Hinkley, R. Pfaffner, S. Niu, J. Li, J. Claverie, Z. Wang, J. Chang, P.M. Fox, Z. Bao, Biodegradable and flexible arterial-pulse sensor for the wireless monitoring of blood flow, *Nat. Biomed. Eng.* 3 (1) (2019) 47–57, <https://doi.org/10.1038/s41551-018-0336-5>.
- [3] J. Gu, Y. Tomioka, K. Kida, Y. Xiao, I. Saito, M. Okazaki, T. Someya, M. Sekino, Measurement of optical reflection and temperature changes after blood occlusion using a wearable device, *Sci. Rep.* 10 (1) (2020), 11491, <https://doi.org/10.1038/s41598-020-68152-6>.
- [4] N. Khatri, S. Zhang, S.S. Kale, Current techniques for postoperative monitoring of microvascular free flaps, *J. Wound, Ostomy Cont. Nurs.* 44 (2) (2017) 148–152, <https://doi.org/10.1097/won.0000000000000314>.
- [5] R. Kraemer, J. Lorenzen, K. Knobloch, S. Papst, M. Kabbani, S. Koennecker, P. M. Vogt, Free flap microcirculatory monitoring correlates to free flap temperature assessment, *J. Plast. Reconstr. Aesthetic Surg.* 64 (10) (2011) 1353–1358, <https://doi.org/10.1016/j.jbjs.2011.04.030>.
- [6] C.J. Salgado, S.L. Moran, S. Mardini, Flap monitoring and patient management, *Plast. Reconstr. Surg.* 124 (6 Suppl) (2009) e295–e302, <https://doi.org/10.1097/PRS.0b013e3181bcf07b>.
- [7] D.L. Cao, X. Chen, F. Cao, W. Guo, J.Y. Tang, C.Y. Cai, S.Q. Cui, X.W. Yang, L. Yu, Y. Su, J.D. Ding, An intelligent transdermal formulation of ALA-loaded copolymer thermogel with spontaneous asymmetry by using temperature-induced sol-gel transition and gel-sol (suspension) transition on different sides, *Adv. Funct. Mater.* 31 (22) (2021), <https://doi.org/10.1002/adfm.202100349>.
- [8] Y.J. Kim, Y.T. Matsunaga, Thermo-responsive polymers and their application as smart biomaterials, *J. Mater. Chem. B* 5 (23) (2017) 4307–4321, <https://doi.org/10.1039/c7tb00157f>.
- [9] F. Rong, T. Wang, Q. Zhou, H. Peng, J. Yang, Q. Fan, P. Li, Intelligent polymeric hydrogen sulfide delivery systems for therapeutic applications, *Bioact. Mater.* 19 (2023) 198–216, <https://doi.org/10.1016/j.bioactmat.2022.03.043>.
- [10] L.L. Jin, Z.X. Zhu, L.J. Hong, Z.F. Qian, F. Wang, Z.W. Mao, ROS-responsive 18 beta-glycyrrhetic acid-conjugated polymeric nanoparticles mediate neuroprotection in ischemic stroke through HMGB1 inhibition and microglia polarization regulation, *Bioact. Mater.* 19 (2023) 38–49, <https://doi.org/10.1016/j.bioactmat.2022.03.040>.
- [11] A.G. Kurian, R.K. Singh, K.D. Patel, J.H. Lee, H.W. Kim, Multifunctional GelMA platforms with nanomaterials for advanced tissue therapeutics, *Bioact. Mater.* 8 (2022) 267–295, <https://doi.org/10.1016/j.bioactmat.2021.06.027>.
- [12] A. Gandhi, A. Paul, S.O. Sen, K.K. Sen, Studies on thermoresponsive polymers: phase behaviour, drug delivery and biomedical applications, *Asian J. Pharm.* 10 (2) (2015) 99–107, <https://doi.org/10.1016/j.ajps.2014.08.010>.
- [13] M. Sponchioni, U.C. Palmiero, D. Moscatelli, Thermo-responsive polymers: applications of smart materials in drug delivery and tissue engineering, *Sci. Eng. C-Mater* 102 (2019) 589–605, <https://doi.org/10.1016/j.msec.2019.04.069>.
- [14] P. Zarrintaj, M. Jouyandeh, M.R. Ganjali, B.S. Hadavand, M. Mozafari, S.S. Sheiko, M. Vatankeh-Varnosfaderani, T.J. Gutierrez, M.R. Saeb, Thermo-sensitive polymers in medicine: a review, *Eur. Polym. J.* 117 (2019) 402–423, <https://doi.org/10.1016/j.eurpolymj.2019.05.024>.
- [15] F. Doberenz, K. Zeng, C. Willems, K. Zhang, T. Groth, Thermoresponsive polymers and their biomedical application in tissue engineering - a review, *J. Mater. Chem. B* 8 (4) (2020) 607–628, <https://doi.org/10.1039/c9tb02052g>.
- [16] M.Q. Le, W. Huang, K.F. Chen, C.H. Lin, L.L. Cai, H.T. Zhang, Y.G. Jia, Upper critical solution temperature polymeric drug carriers, *Chem. Eng. J.* 432 (2022), <https://doi.org/10.1016/j.cej.2021.134354>.
- [17] L. Zhou, C. Dai, L. Fan, Y.H. Jiang, C. Liu, Z.N. Zhou, P.F. Guan, Y. Tian, J. Xing, X. J. Li, Y.A. Luo, P. Yu, C.Y. Ning, G.X. Tan, Injectable self-healing natural biopolymer-based hydrogel adhesive with thermoresponsive reversible adhesion for minimally invasive surgery, *Adv. Funct. Mater.* 31 (14) (2021), <https://doi.org/10.1002/adfm.202007457>.
- [18] R. Laurano, M. Boffito, M. Abrami, M. Grassi, A. Zoso, V. Chiono, G. Ciardelli, Dual stimuli-responsive polyurethane-based hydrogels as smart drug delivery carriers for the advanced treatment of chronic skin wounds, *Bioact. Mater.* 6 (9) (2021) 3013–3024, <https://doi.org/10.1016/j.bioactmat.2021.01.0003>.
- [19] Q. Lv, C.L. He, F.L. Quan, S.J. Yu, X.S. Chen, DOX/IL-2/IFN-gamma co-loaded thermo-sensitive polypeptide hydrogel for efficient melanoma treatment, *Bioact. Mater.* 3 (1) (2018) 118–128, <https://doi.org/10.1016/j.bioactmat.2017.08.003>.
- [20] F. Yang, K. Shi, Y. Hao, Y. Jia, Q. Liu, Y. Chen, M. Pan, L. Yuan, Y. Yu, Z. Qian, Cyclophosphamide loaded thermo-responsive hydrogel system synergize with a hydrogel cancer vaccine to amplify cancer immunotherapy in a prime-boost manner, *Bioact. Mater.* 6 (10) (2021) 3036–3048, <https://doi.org/10.1016/j.bioactmat.2021.03.003>.
- [21] Y. Han, L. Jiang, H. Shi, C. Xu, M. Liu, Q. Li, L. Zheng, H. Chi, M. Wang, Z. Liu, M. You, X.J. Loh, Y.L. Wu, Z. Li, C. Li, Effectiveness of an ocular adhesive polyhedral oligomeric silsesquioxane hybrid thermo-responsive FK506 hydrogel in a murine model of dry eye, *Bioact. Mater.* 9 (2022) 77–91, <https://doi.org/10.1016/j.bioactmat.2021.07.027>.
- [22] Y. Ma, Y. Yin, L. Ni, H. Miao, Y. Wang, C. Pan, X. Tian, J. Pan, T. You, B. Li, G. Pan, Thermo-responsive imprinted hydrogel with switchable sialic acid recognition for selective cancer cell isolation from blood, *Bioact. Mater.* 6 (5) (2021) 1308–1317, <https://doi.org/10.1016/j.bioactmat.2020.10.008>.
- [23] F.Y. Zhou, B. Feng, T.T. Wang, D.G. Wang, Q.S. Meng, J.F. Zeng, Z.W. Zhang, S. L. Wang, H.J. Yu, Y.P. Li, Programmed multiresponsive vesicles for enhanced tumor penetration and combination therapy of triple-negative breast cancer, *Adv. Funct. Mater.* 27 (20) (2017), <https://doi.org/10.1002/adfm.201606530>.
- [24] J.F. Ji, F. Ma, H.B. Zhang, F.Y. Liu, J. He, W.L. Li, T.T. Xie, D.N. Zhong, T.T. Zhang, M. Tian, H. Zhang, H.A. Santos, M. Zhou, Light-activatable Assembled nanoparticles to improve tumor penetration and eradicate metastasis in triple negative breast cancer, *Adv. Funct. Mater.* 28 (33) (2018), <https://doi.org/10.1002/adfm.201801738>.

- [25] S.Y. Turin, R.L. Walton, G.A. Dumanian, J.B. Hijawi, J.A. LoGiudice, M. Alghoul, Current practices in the management of postoperative arterial vasospasm in microsurgery, *J. Reconstr. Microsurg.* 34 (4) (2018) 242–249, <https://doi.org/10.1055/s-0037-1612601>.
- [26] M. Saint-Cyr, C. Wong, E.W. Buchel, S. Colohan, W.C. Pederson, Free tissue transfers and replantation, *Plast. Reconstr. Surg.* 130 (6) (2012) 858e–878e, <https://doi.org/10.1097/PRS.0b013e31826da2b7>.
- [27] G.G. Hallock, The complete classification of flaps, *Microsurg* 24 (3) (2004) 157–161, <https://doi.org/10.1002/micr.20035>.
- [28] J. Shi, L. Yu, J. Ding, PEG-based thermosensitive and biodegradable hydrogels, *Acta Biomater.* 128 (2021) 42–59, <https://doi.org/10.1016/j.actbio.2021.04.009>.
- [29] Y.P. Zhuang, X.W. Yang, Y.M. Li, Y.P. Chen, X.C. Peng, L. Yu, J.D. Ding, Sustained release strategy designed for lixisenatide delivery to synchronously treat diabetes and associated complications, *ACS Appl. Mater. Interfaces* 11 (33) (2019) 29604–29618, <https://doi.org/10.1021/acami.9b10346>.
- [30] M.S. Shim, H.T. Lee, W.S. Shim, I. Park, H. Lee, T. Chang, S.W. Kim, D.S. Lee, Poly(D,L-lactic acid-co-glycolic acid)-b-poly(ethylene glycol)-b-poly(D,L-lactic acid-co-glycolic acid) triblock copolymer and thermoreversible phase transition in water, *J. Biomed. Mater. Res.* 61 (2) (2002) 188–196, <https://doi.org/10.1002/jbm.10164>.
- [31] L. Yu, G.T. Chang, H. Zhang, J.D. Ding, Temperature-induced spontaneous sol-gel transitions of poly(D,L-lactic acid-co-glycolic acid)-b-poly(ethylene glycol)-b-poly(D,L-lactic acid-co-glycolic acid) triblock copolymers and their end-capped derivatives in water, *J. Polym. Sci., Polym. Chem. Ed.* 45 (6) (2007) 1122–1133, <https://doi.org/10.1002/pola.21876>.
- [32] B. Jeong, Y.H. Bae, S.W. Kim, Thermoreversible gelation of PEG–PLGA–PEG triblock copolymer aqueous solutions, *Macromolecules* 32 (21) (1999) 7064–7069, <https://doi.org/10.1021/ma9908999>.
- [33] S.J. Bae, J.M. Suh, Y.S. Sohn, Y.H. Bae, S.W. Kim, B. Jeong, Thermogelling poly(caprolactone-b-ethylene glycol-b-caprolactone) aqueous solutions, *Macromolecules* 38 (12) (2005) 5260–5265, <https://doi.org/10.1021/ma050489m>.
- [34] L. Chen, T. Ci, T. Li, L. Yu, J. Ding, Effects of molecular weight distribution of amphiphilic block copolymers on their solubility, micellization, and temperature-induced sol gel transition in water, *Macromolecules* 47 (17) (2014) 5895–5903, <https://doi.org/10.1021/ma501110p>.
- [35] L. Chen, T. Ci, L. Yu, J. Ding, Effects of molecular weight and its distribution of PEG block on micellization and thermogellability of PLGA-PEG-PLGA copolymer aqueous solutions, *Macromolecules* 48 (11) (2015) 3662–3671, <https://doi.org/10.1021/acs.macromol.5b00168>.
- [36] R. Wang, X. Yao, T. Li, X. Li, M. Jin, Y. Ni, W. Yuan, X. Xie, L. Lu, M. Li, Reversible thermoresponsive hydrogel fabricated from natural biopolymer for the improvement of critical limb ischemia by controlling release of stem cells, *Adv. Healthc. Mater.* 8 (20) (2019), e1900967, <https://doi.org/10.1002/adhm.201900967>.
- [37] Z. Xing, C. Zhao, S. Wu, D. Yang, C. Zhang, X. Wei, X. Wei, H. Su, H. Liu, Y. Fan, Hydrogel loaded with VEGF/TFEB-Engineered extracellular vesicles for rescuing critical limb ischemia by a dual-pathway activation strategy, *Adv. Healthc. Mater.* 11 (5) (2022), e2100334, <https://doi.org/10.1002/adhm.202100334>.
- [38] K.T. Chen, S. Mardini, D.C. Chuang, C.H. Lin, M.H. Cheng, Y.T. Lin, W.C. Huang, C. K. Tsao, F.C. Wei, Timing of presentation of the first signs of vascular compromise dictates the salvage outcome of free flap transfers, *Plast. Reconstr. Surg.* 120 (1) (2007) 187–195, <https://doi.org/10.1097/01.prs.0000264077.07779.50>.
- [39] D. Zheng, W. Chen, H. Ruan, Z. Cai, X. Chen, T. Chen, Y. Zhang, W. Cui, H. Chen, H. Shen, Metformin-hydrogel with glucose responsiveness for chronic inflammatory suppression, *Chem. Eng. J.* 428 (2022), <https://doi.org/10.1016/j.cej.2021.131064>.
- [40] Y.P. Zhuang, H. Shen, F. Yang, X. Wang, D.C. Wu, Synthesis and characterization of PLGA nanoparticle/4-arm-PEG hybrid hydrogels with controlled porous structures, *RSC Adv.* 6 (59) (2016) 53804–53812, <https://doi.org/10.1039/c6ra08404d>.
- [41] L.W. Hong, G.X. Chen, Z.W. Cai, H. Liu, C. Zhang, F. Wang, Z.Y. Xiao, J. Zhong, L. Wang, Z.T. Wang, W.G. Cui, Balancing microthrombosis and inflammation via injectable protein hydrogel for inflammatory bowel disease, *Adv. Sci.* 9 (20) (2022), 2200281, <https://doi.org/10.1002/advs.202200281>.
- [42] L. Chen, L. Cheng, Z. Wang, J. Zhang, X. Mao, Z. Liu, Y. Zhang, W. Cui, X. Sun, Conditioned medium-electrospun fiber biomaterials for skin regeneration, *Bioact. Mater.* 6 (2) (2021) 361–374, <https://doi.org/10.1016/j.bioactmat.2020.08.022>.
- [43] X. Wang, W.S. Cheang, H. Yang, L. Xiao, B. Lai, M. Zhang, J. Ni, Z. Luo, Z. Zhang, Y. Huang, N. Wang, Nuciferine relaxes rat mesenteric arteries through endothelium-dependent and -independent mechanisms, *Br. J. Pharmacol.* 172 (23) (2015) 5609–5618, <https://doi.org/10.1111/bph.13021>.
- [44] W.S. Cheang, M.Y. Lam, W.T. Wong, X.Y. Tian, C.W. Lau, Z. Zhu, X. Yao, Y. Huang, Menthol relaxes rat aortae, mesenteric and coronary arteries by inhibiting calcium influx, *Eur. J. Pharmacol.* 702 (1–3) (2013) 79–84, <https://doi.org/10.1016/j.ejphar.2013.01.028>.
- [45] T. Luo, Z. Chen, F. Wang, S. Yin, P. Liu, J. Zhang, Z. Yang, Endothelium-independent vasodilatory effects of isodilapolyglycol isolated from ostericum citridorum, *Molecules* 25 (4) (2020), <https://doi.org/10.3390/molecules25040885>.
- [46] M.C. Edmunds, S. Wigmore, D. Kluth, In situ transverse rectus abdominis myocutaneous flap: a rat model of myocutaneous ischemia reperfusion injury, *Jove-J Vis Exp* 76 (2013), <https://doi.org/10.3791/50473>.
- [47] O. Ergun, F. Yuksel, E. Ulkur, B. Celikoz, Effect of hydrostatic dilation on flap viability of the transverse rectus abdominis musculocutaneous flap model in rats, *Plast. Reconstr. Surg.* 120 (1) (2007) 68–77, <https://doi.org/10.1097/01.prs.0000263334.84485.34>.
- [48] B. Ersoy, O. Cevik, O.T. Cilingir, Etanercept protects myocutaneous flaps from ischaemia reperfusion injury: an experimental study in a rat tram flap model, *J. Plast. Surg. Hand Surg.* 50 (4) (2016) 208–215, <https://doi.org/10.3109/2006656x.2016.1151437>.
- [49] E. Komorowska-Timek, S.G. Chen, F. Zhang, T. Dogan, W.C. Lineaweaver, H. J. Buncke, Prolonged perivascular use of verapamil or lidocaine decreases skin flap necrosis, *Ann. Plast. Surg.* 43 (3) (1999) 283–288, <https://doi.org/10.1097/00006637-199909000-00010>.
- [50] N. Weinzweig, F. Lukash, J. Weinzweig, Topical and systemic calcium channel blockers in the prevention and treatment of microvascular spasm in a rat epigastric island skin flap model, *Ann. Plast. Surg.* 42 (3) (1999) 320–326, <https://doi.org/10.1097/00006637-199903000-00015>.
- [51] W. Zhu, S. Liu, J. Zhao, S. Liu, S. Jiang, B. Li, H. Yang, C. Fan, W. Cui, Highly flexible and rapidly degradable papaverine-loaded electrospun fibrous membranes for preventing vasospasm and repairing vascular tissue, *Acta Biomater.* 10 (7) (2014) 3018–3028, <https://doi.org/10.1016/j.actbio.2014.03.023>.
- [52] X.X. Tao, S.M. Wu, D.S. Lin, Effects of vinpocetine on random skin flap survival in rats, *J. Reconstr. Microsurg.* 29 (6) (2013) 393–397, <https://doi.org/10.1055/s-0033-1343834>.
- [53] A. Gurlek, M. Celik, H. Parlakpınar, H. Aydoğan, A. Bay-Karabulut, The protective effect of melatonin on ischemia-reperfusion injury in the groin (inferiorepigastric) flap model in rats, *J. Pineal Res.* 40 (4) (2006) 312–317, <https://doi.org/10.1111/j.1600-079X.2006.00319.x>.
- [54] L. Zhang, L. Chen, Y. Xiang, Z. Liu, X. Mao, L. Zhang, L. Deng, Y. Zhang, L. Cheng, X. Sun, W. Cui, Multifunctional integrally-medicalized hydrogel system with internal synergy for efficient tissue regeneration, *Chem. Eng. J.* 406 (2021), <https://doi.org/10.1016/j.cej.2020.126839>.
- [55] P. Hyza, L. Streit, D. Schwarz, T. Kubek, J. Vesely, Vasospasm of the flap pedicle: the effect of 11 of the most often used vasodilating drugs. Comparative study in a rat model, *Plast. Reconstr. Surg.* 134 (4) (2014) 574e–584e, <https://doi.org/10.1097/prs.0000000000000570>.
- [56] I.Y. Kuo, B.E. Ehrlich, Signaling in muscle contraction, *Cold Spring Harbor Perspect. Biol.* 7 (2) (2015), <https://doi.org/10.1101/cshperspect.a006023>.
- [57] L. Shaw, S. O'Neill, C.J.P. Jones, C. Austin, M.J. Taggart, Comparison of U46619-, endothelin-1- or phenylephrine-induced changes in cellular Ca<sup>2+</sup> profiles and Ca<sup>2+</sup> sensitisation of constriction of pressurised rat resistance arteries, *Br. J. Pharmacol.* 141 (4) (2004) 678–688, <https://doi.org/10.1038/sj.bjp.0705647>.
- [58] C.H. Lee, D. Poburko, P. Sahota, J. Sandhu, D.O. Ruehlmann, C. van Breeman, The mechanism of phenylephrine-mediated Ca<sup>2+</sup> (i) oscillations underlying tonic contraction in the rabbit inferior vena cava, *J. Physiol. Lond.* 534 (3) (2001) 641–650, <https://doi.org/10.1111/j.1469-7793.2001.t01-1-00641.x>.
- [59] Z. Liu, B. Zhao, L. Zhang, S. Qian, J. Mao, L. Cheng, X. Mao, Z. Cai, Y. Zhang, W. Cui, X. Sun, Modulated integrin signaling receptors of stem cells via ultra-soft hydrogel for promoting angiogenesis, *Compos. B Eng.* 234 (2022), 109747, <https://doi.org/10.1016/j.compositesb.2022.109747>.
- [60] X.Y. Mao, R.Y. Cheng, H.B. Zhang, J.H. Bae, L.Y. Cheng, L. Zhang, L.F. Deng, W. G. Cui, Y.G. Zhang, H.A. Santos, X.M. Sun, Self-healing and injectable hydrogel for matching skin flap regeneration, *Adv. Sci.* 6 (3) (2019), 1801555, <https://doi.org/10.1002/advs.201801555>.
- [61] L. Zhang, Y. Xiang, H. Zhang, L. Cheng, X. Mao, N. An, L. Zhang, J. Zhou, L. Deng, Y. Zhang, X. Sun, H.A. Santos, W. Cui, A biomimetic 3D-self-forming approach for microvascular scaffolds, *Adv. Sci.* 7 (9) (2020), 1903553, <https://doi.org/10.1002/advs.201903553>.
- [62] H. Kawabata, K.R. Knight, S.A. Coe, J.A. Angus, B.M. O'Brien, Experience with calcium antagonists nitrendipine, diltiazem, and verapamil and beta 2-agonists-albutamol in salvaging ischemic skin flaps in rabbits, *Microsurg* 12 (3) (1991) 160–163, <https://doi.org/10.1002/micr.1920120303>.
- [63] G. Zavitsanos, L. Huang, W. Panza, D. Serafin, B. Klitzman, Limiting impairment of muscle function following ischemia and reperfusion in rabbits, *J. Reconstr. Microsurg.* 12 (3) (1996) 183–187, <https://doi.org/10.1055/s-2007-1006474>.
- [64] T. Fukai, M. Ushio-Fukai, Superoxide dismutases: role in redox signaling, vascular function, and diseases, *Antioxid. Redox Signal.* 15 (6) (2011) 1583–1606, <https://doi.org/10.1089/ars.2011.3999>.
- [65] A. Gurlek, M. Celik, H. Parlakpınar, H. Aydoğan, A. Bay-Karabulut, The protective effect of melatonin on ischemia-reperfusion injury in the groin (inferior epigastric) flap model in rats, *J. Pineal Res.* 40 (4) (2006) 312–317, <https://doi.org/10.1111/j.1600-079X.2006.00319.x>.
- [66] D.R. Janero, Malondialdehyde and thiobarbituric acid-reactivity as diagnostic indices of lipid peroxidation and peroxidative tissue injury, *Free Radic. Biol. Med.* 9 (6) (1990) 515–540, [https://doi.org/10.1016/0891-5849\(90\)90131-2](https://doi.org/10.1016/0891-5849(90)90131-2).
- [67] B. Kalyanaram, Teaching the basics of redox biology to medical and graduate students: oxidants, antioxidants and disease mechanisms, *Redox Biol.* 1 (1) (2013) 244–257, <https://doi.org/10.1016/j.redox.2013.01.014>.
- [68] E. Ho, K.K. Galougahi, C.C. Liu, R. Bhandi, G.A. Figtree, Biological markers of oxidative stress: applications to cardiovascular research and practice, *Redox Biol.* 1 (1) (2013) 483–491, <https://doi.org/10.1016/j.redox.2013.07.006>.
- [69] R.J. Carpenter, M.F. Angel, L.R. Amis, T.M. Masterson, R.F. Morgan, Verapamil enhances the survival of primary ischemic venous obstructed rodent skin flaps, *Arch. Otolaryngol. Head Neck Surg.* 119 (9) (1993) 1015–1017, <https://doi.org/10.1001/archotol.1993.01880210105014>.
- [70] L. Yu, Z. Zhang, H. Zhang, J. Ding, Biodegradability and biocompatibility of thermoreversible hydrogels formed from mixing a sol and a precipitate of block copolymers in water, *Biomacromolecules* 11 (8) (2010) 2169–2178, <https://doi.org/10.1021/bm100549q>.
- [71] X. Chen, J. Zhang, K. Wu, X. Wu, J. Tang, S. Cui, D. Cao, R. Liu, C. Peng, L. Yu, J. Ding, Visualizing the in vivo evolution of an injectable and thermosensitive

hydrogel using tri-modal bioimaging, *Small Methods* 4 (9) (2020), 2000310, <https://doi.org/10.1002/smt.202000310>.